Bull. Mater. Sci., Vol. 22, No. 3, May 1999, pp. 265–274. © Indian Academy of Sciences.

Study of the impact of HgO addition and low-field magnetic relaxation behaviour in granular high-T_c superconductors

R G SHARMA*, S LAHIRY, A PANDEY and DIPTEN BHATTACHARYA
National Physical Laboratory, New Delhi 110 012, India

Abstract. A series of high-T_c superconductors have been prepared with the HgO addition/substitution. Significant improvement in the T_{conset} as well as T_{c0} was observed in all the cases. Substitution of Hg at the Sr site and Ba site in the case of (Bi, Pb)–Sr–Ca–Cu–O and Y–Ba–Cu–O systems, respectively over a range 0·01–0·6 at% helps in constructing an entire spectrum: improvement of T_{c0} up to 0·4 at% in the case of Bi-system and up to 0·03 at% in the case of Y123 system and slight drop in T_c thereafter. Such improvement is the result of abundant supply of highly reactive nascent oxygen all through the bulk. HgO decomposes and provides oxygen which helps in maintaining proper oxygen stoichiometry throughout the bulk. No Hg or Hg-based impure phases were observed in the X-ray diffraction spectra. Low-field (10–100 Oe) magnetic relaxation studies reveal faster relaxation of the intergranular critical state in the case of silver added samples as the grain boundary coupling energy E_J becomes quite uniform across the entire bulk which leads to smaller flux pinning energy. The distribution of the pinning energy is evaluated from the observed relaxation pattern and is found to be narrower in the case of silver added samples. It was also observed that the transport $J_c \sim \exp[-\Delta T_c/T_{c0}]$ and the flux pinning energy $U \sim \Delta T_c$, where ΔT_c is the transition width and is a measure of the inhomogeneity within the sample. Such relationships may help in devising a strategy for achieving high J_c, high U yet low ΔT_c. Silver addition turns out to be an effective tool in tailoring the sample properties depending on requirement.

Keywords. Hg addition; oxygen source; magnetic relaxation; grain boundary coupling energy; flux pinning energy.

1. Introduction

Ever since the Hg-based new high-T_c superconductor systems—$HgBa_2CuO_{4-\delta}$ (Hg-1201), $HgBa_2CaCu_2O_{6-\delta}$ (Hg-1212), and $HgBa_2Ca_2Cu_3O_{8-\delta}$ (Hg-1223)—were discovered (Putilin *et al* 1993; Schilling *et al* 1993), there has been a renewed interest in the role of Hg in this class of materials. The enhancement of T_c is certainly a major stimulant which prompted exploration of the role of Hg in more commonly used high-T_c systems, namely, Y–Ba–Cu–O (YBCO) and Bi–Sr–Ca–Cu–O (BSCCO), as well. Comprehensive studies have been carried out by our group in this context which will be reviewed in this paper. We have substituted Hg at suitable sites as well as added HgO in otherwise stoichiometric composition. We have observed interesting results in both the cases which prompted us to propose such substitution/addition as a viable technique for improvement of all round properties of the high-T_c superconductors. HgO is found to be an abundant source of nascent oxygen within the high-T_c superconductors which helps maintain proper oxygen stoichiometry within the lattice. It is possible to observe T_{conset} as high as 135 K (Lahiry *et al* 1994) and $T_{c0} \sim 114$ K in a composition $Bi_{1.7}Pb_{0.3}Sr_{2-x}Hg_xCa_2Cu_3O_y$ (BPSCCO) for $x = 0.4$ and 0·3, respectively. In YBCO system too, substitution and addition of HgO leads to a well oxygenated stoichiometric material with a $T_{c0} = 91$ K (Pandey *et al* 1996, 1997). All the specimens are calcined and sintered in air. Oxygen stoichiometry is found to be uniform throughout the bulk. Addition of HgO to the other RE–Ba–Cu–O (RE = rare-earth) systems is also found to be quite useful as it does away with the requirement of flowing oxygen during sintering.

We have studied the intergranular flux creeping and consequent low-field magnetic relaxation in such granular high-T_c systems. The parent ceramic system exhibits slower relaxation of the intergranular critical state than the intragranular relaxation. The silver added samples, on the other hand, show faster relaxation. This observation can be understood from the fact that the flux pinning in a disordered Josephson junction array (which truly resembles the granular medium) depends on the variation of the Josephson coupling energy E_J across the entire array. Parent ceramic system possesses large variation in E_J which leads to high flux pinning barrier U. The consequence is slower rate of flux creeping and hence magnetic relaxation. Silver addition gives rise to a uniformity in the grain boundary characteristics which, in turn, reduces the degree of variation in E_J. The flux pinning energy U, therefore, becomes small in silver added samples which leads to faster relaxation of the intergranular critical state. Consequence of all these in

*Author for correspondence

the context of critical current of the granular medium is discussed in this paper.

The entire paper is divided into two broad sections: § 2 describes the results regarding the role of HgO in high-T_c superconducting systems and § 3 describes the results regarding the relaxation studies at low field.

2. Role of HgO in high-T_c superconductors

HgO is added to the bulk YBCO and BPSCCO superconducting systems during processing of the materials. A large number of samples with different levels of HgO have been prepared to observe the impact of (i) substitution of Str-site in BPSCCO and Ba-site in YBCO by Hg; (ii) addition of HgO to stoichiometric YBCO; (iii) addition of HgO along with Ag or Ag_2O to YBCO; (iv) addition of HgO in the entire family of RE–Ba–Cu–O superconductors. In almost all the cases significant improvement in the superconducting transition has been observed. Of course, it appears that there is an optimum level of HgO addition beyond which the overall superconductivity starts degrading a little. In the following paragraphs results regarding the BPSCCO, YBCO, RE–Ba–Cu–O, and Ag added high-T_c systems are discussed.

2.1 *The $(Bi, Pb)_2Sr_{2-x}Hg_xCa_2Cu_3O_y$ system*

Samples with nominal composition $Bi_{1.7}Pb_{0.3}Sr_{2-x}Hg_x$-$Ca_2Cu_3O_y$, $x = 0.0$, 0.2, 0.3, 0.4, 0.6, 1.0, have been prepared by standard solid state reaction route (Lahiry *et al* 1994). All the ingredients are mixed in stoichiometric proportion and the mixture is calcined thrice at 820°C for 15 h and 54 h in air. The temperature is raised in steps (avoiding fast heating rate) in order to prevent melting of the low melting point oxides. The calcined product is compacted into pellets and sintered at 820°C for 65 h. The resistivity is measured by standard four-probe technique while the ac susceptibility is measured by mutual inductance technique using a lock-in amplifier system.

Figure 1 is a plot of normalized resistivity vs temperature for all the specimens. The highest T_{conset} of 135 K is observed in the case of the sample with $x = 0.4$ even though the transition is quite broad. Sharpest transition is observed for $x = 0.3$ with $T_{conset} = 120$ K and $T_{c0} = 114$ K. For the samples with $x > 0.3$, T_{c0} decreases. The susceptibility results (figure 2) are also in agreement with the resistivity data. The room temperature X-ray diffraction spectra (figure 3) for all these samples exhibit pure 2212 phase without any reflection corresponding to the Hg or Hg-based compounds. This observation, therefore, is quite surprising as unusually high T_c is observed in 2212 phase. We have examined the reproducibility of the results and they are found to be consistent in all the trials. Since HgO dissociates at a temperature ~ 476°C, nascent oxygen is available all through the bulk. Moreover, Hg is substituted at the Sr site and since Hg is evaporated there are vacancies at the Sr-site which leads to the lattice distortion as well as excess oxygen in the Sr–O plane. Such effects might have influenced the charge carrier concentration and the super-carrier formation which, in turn, has given rise to

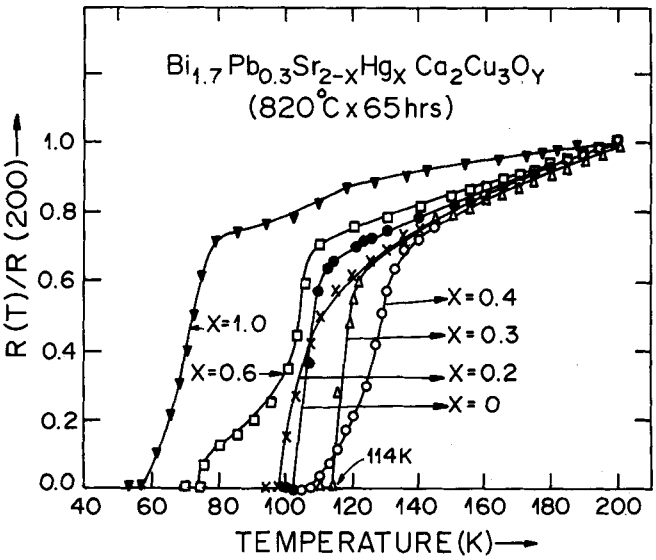

Figure 1. Normalized resistance of $Bi_{1.7}Pb_{0.3}Sr_{2-x}Hg_xCa_2Cu_3O_y$ specimens ($x = 0.0$, 0.2, 0.3, 0.4, 0.6 and 1.0) plotted against temperature. Highest $T_{conset} \sim 135$ K is observed for $x = 0.4$ and highest $T_{c0} \sim 114$ K for $x = 0.3$ specimen (Lahiry *et al* 1994).

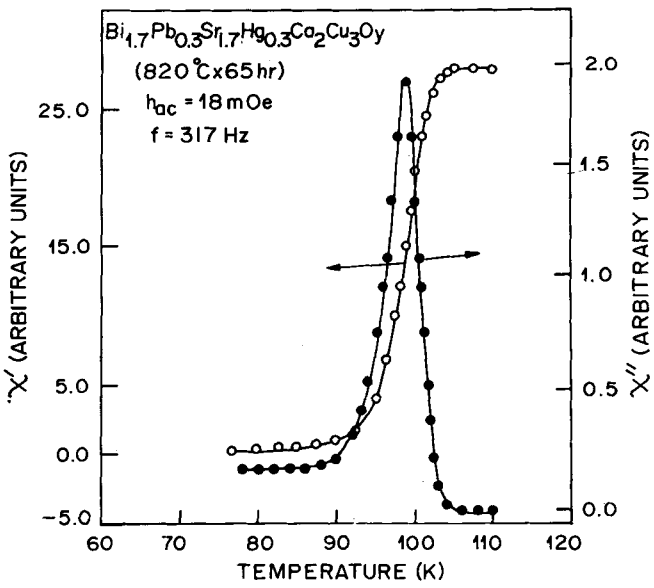

Figure 2. The real (χ') and imaginary (χ'') parts of ac susceptibility vs temperature plots for $Bi_{1.7}Pb_{0.3}Sr_{2-x}Hg_xCa_2Cu_3O_y$ specimens for $x = 0.3$. An excitation field of 18 mOe and a frequency of 317 Hz are used. The χ''–T peak is sharp and close to the χ'–T diamagnetic transition peak (Lahiry *et al* 1994).

unusually high T_c. It has indeed been observed in a separate study that the T_c improves steadily if the Sr stoichiometry is brought down from 2·0 to 1·6.

2.2 *The $YBa_{2-x}Hg_xCu_3O_{7-\delta}$ system*

The oxygen stoichiometry in the Y–Ba–Cu–O system governs the T_c significantly. Therefore, it is important to maintain proper oxygen stoichiometry within the lattice. In the specimens prepared by conventional technique, a drop in oxygen stoichiometry and a consequent drop in T_c is observed as one measures the T_c from the surface to the bulk even if the specimens are sintered in flowing oxygen. Conder *et al* (1989) were able to improve the uniformity of oxygen distribution by optimizing the heating rate and following a cumbersome annealing–grinding procedure. HgO addition or substitution turns out to be an excellent technique in this regard which produces very good quality superconducting samples without any flow of oxygen (Pandey *et al* 1996). Simple air sintered samples exhibit $T_c \sim 91$ K. The oxygen stoichiometry is found to be uniform too, all through the bulk.

Samples with nominal composition $YBa_{2-x}Hg_xCu_3O_{7-\delta}$ ($x = 0{\cdot}01, 0{\cdot}03, 0{\cdot}1, 0{\cdot}2, 0{\cdot}3$ and $0{\cdot}4$) have been prepared by solid state reaction technique. The mixture of the ingredients is calcined at 700°C for 16 h. The product is calcined twice at 800°C for 16 h with intermediate grinding. Calcined material is finally ground and compacted in the form of pellets which are then sintered at 875°C for 16 h in air.

Figure 4 depicts the normalized resistance vs temperature for the samples with $x = 0{\cdot}01$, $0{\cdot}03$, $0{\cdot}1$, $0{\cdot}2$, $0{\cdot}3$ and $0{\cdot}4$. The T_{c0} is found to be varying over 90–68 K as x is increased. The width of the transition increases with the increase in x. The degradation of T_{c0} can be understood from the increase in Ba vacancies. As pointed out by Samel *et al* (1995), the bonding between Ba^{2+} and apical O^{2-} helps in charge transfer towards the Cu–O plane which, in turn, increases the charge carrier con-

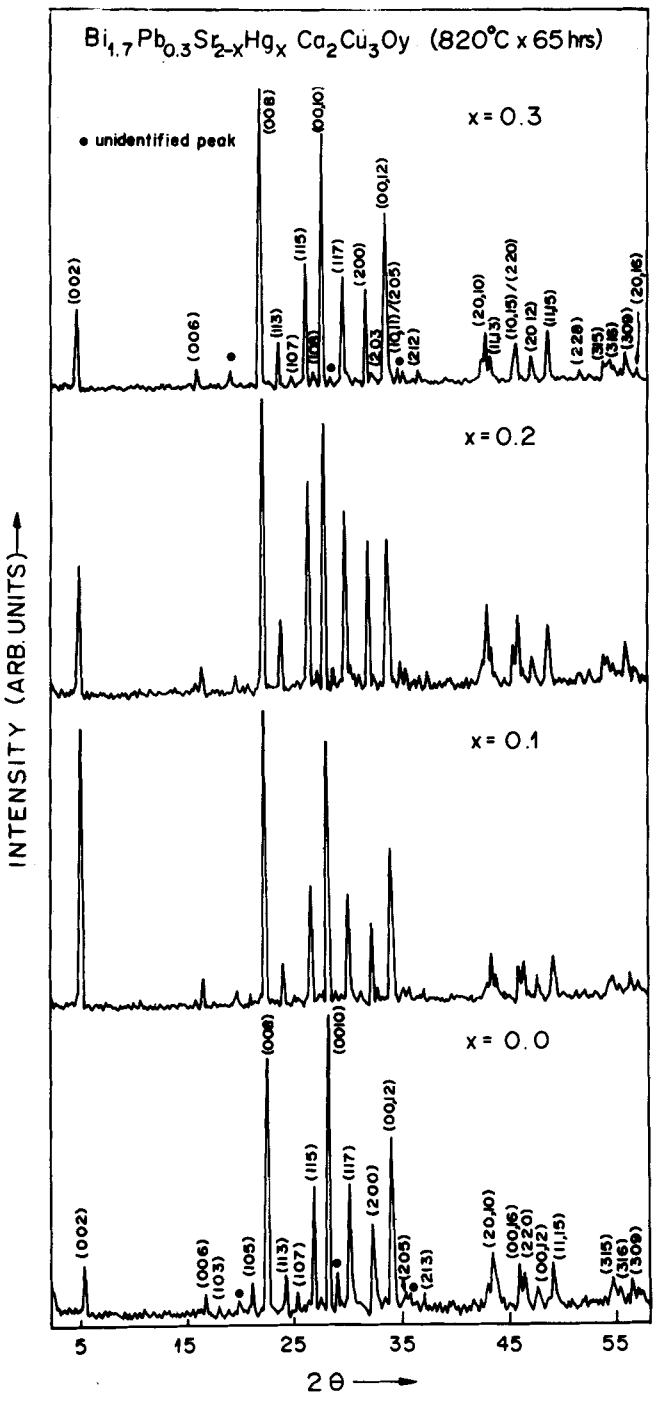

Figure 3. Room temperature X-ray diffraction spectra for $Bi_{1.7}Pb_{0.3}Sr_{2-x}Hg_xCa_2Cu_3O_y$ ($x = 0{\cdot}0$, $0{\cdot}1$, $0{\cdot}2$ and $0{\cdot}3$). All the specimens show predominantly 2212 phase. Some unidentified peaks are shown by dots (Lahiry *et al* 1994).

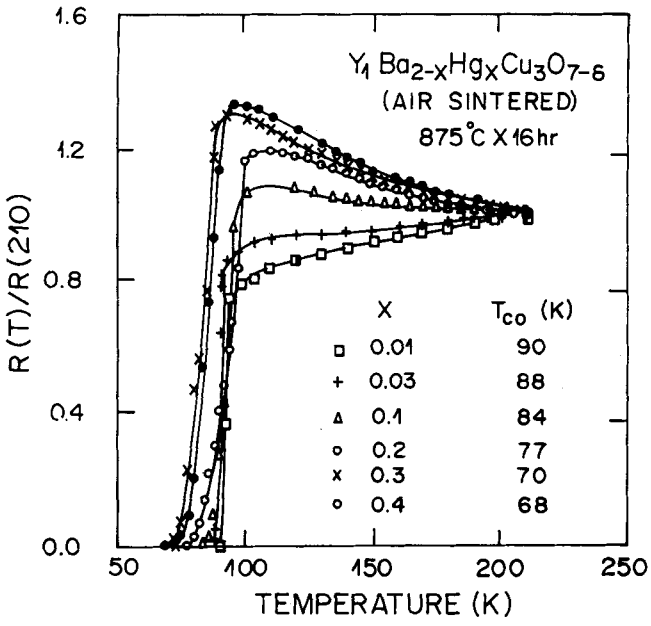

Figure 4. Normalized resistance vs temperature for $YBa_{2-x}Hg_xCu_3O_{7-\delta}$ specimens ($x = 0{\cdot}01$, $0{\cdot}03$ and $0{\cdot}1$ to $0{\cdot}4$). All the samples are sintered in air (Pandey *et al* 1996).

centration. Vacancy at Ba-site, therefore, leads to a decrease in the charge carrier concentration in the Cu–O plane and hence a drop in T_c is observed with the increase in Hg substitution. It turns out that a very small concentration of Hg ($x = 0.01$) is good enough to yield 90 K superconductor. Figure 5 shows the variation of T_{c0} with the Hg concentration.

The XRD spectra (figure 6) exhibit a perfect orthorhombic phase with a few low intensity peaks corresponding to the impure phases like Ba_2CuO_3 and $BaCuO_2$. No reflection corresponding to pure Hg or Hg-based compounds are observed which confirms, once again, that Hg is not retained in the matrix. A striking feature is the maintenance of the proper oxygen stoichiometry all through the bulk. HgO helps in reducing the sintering temperature also, from ~ 920–950°C to 875°C.

2.3 *The $YBa_2Cu_3O_{7-\delta}$ + HgO system*

We have prepared YBCO samples with HgO addition as well. HgO is added in otherwise stoichiometric $YBa_2Cu_3O_{7-\delta}$ composition (Pandey *et al* 1997). Initially, the YBCO compound is formed by solid state reaction technique. After calcination, HgO is added in 0·5, 1·0, 5·0, 10·0 and 20·0 at% and the mixture is calcined again. The calcined product is compacted into pellets which are subsequently sintered at 875°C for 16 h in air.

Figure 7 depicts the normalized resistance vs temperature for all the samples. Specimens with 0·5, 1·0 and 5·0 at% HgO exhibit T_{c0} ~ 90 K while higher HgO addition seems to have given rise to a marginal drop in T_{c0} down to ~ 85 K. The transition width too, in the latter cases is broader which reveals a weak grain to grain coupling. The nature of grain to grain coupling can be observed from the real part of the ac susceptibility vs temperature (χ–T) plots also (figure 8). There are plateaus in the plots for the samples with 10 and 20 at% HgO which reflect poor grain to grain coupling. One of the reasons could be an increased porosity in the samples because of the evaporation of Hg during heat treatment. The scanning electron micrograph (SEM) is shown in figure 9. Uniform distribution of pores could be seen throughout the area. The XRD patterns for three representative samples (with 0·5, 5·0, and 20·0 at% HgO) are shown in figure 10. No change in lattice parameters is observed and no reflection corresponding to Hg or Hg-based compounds could be found. Therefore, it can be asserted conclusively that HgO provides an excellent internal source of highly reactive nascent oxygen which helps in improving the quality of the superconductors and also expedites the processing of the samples. Consistent and sharp T_c ~ 90 K implies that the oxygen stoichiometry is close to 7 and is uniform throughout the entire matrix.

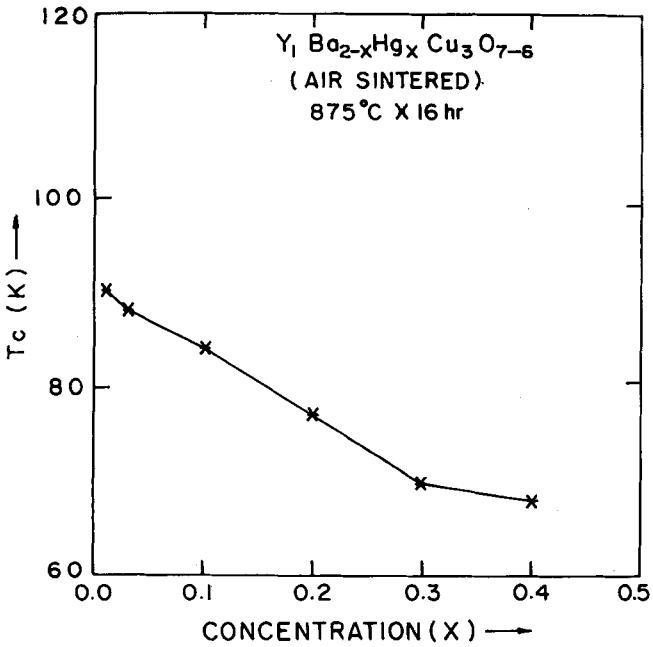

Figure 5. Variation of T_{c0} with Hg concentration (x) in $YBa_{2-x}Hg_xCu_3O_{7-\delta}$ specimens sintered in air (875°C, 16 h) (Pandey *et al* 1996).

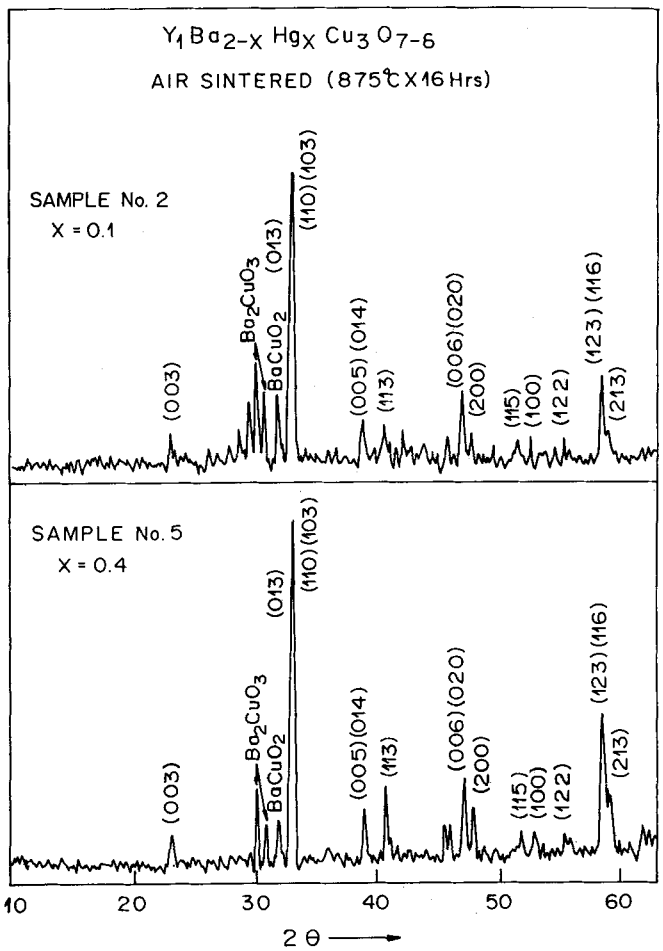

Figure 6. Representative XRD spectra of two specimens $YBa_{2-x}Hg_xCu_3O_{7-\delta}$ ($x = 0.1$ and 0·4). Both the spectra show an orthorhombic phase (Pandey *et al* 1996).

In this context it is worthwhile to mention that Ag_2O too, is known to dissociate at a lower temperature (~ 187°C) and can work as an internal source of oxygen. However, Ag is retained in the matrix which again forms the oxide during cooling (Singh *et al* 1989; Kao *et al* 1990). Therefore, the oxygen stoichiometry is disturbed in the specimens. Hg, on the contrary, is not retained in the matrix and hence proves to be a much more effective internal source of oxygen.

2.4 *The RE–$Ba_2Cu_3O_{7-\delta}$ system*

We extend the studies to the entire family of RE–Ba–Cu–O systems (RE = Dy, Gd, and Eu). Specimens have been prepared by the solid state reaction technique as described in the earlier sub-sections. The basic raw materials are mixed and calcined thrice at 850°C for 16 h with intermediate grinding and finally 1 wt% HgO is added to the calcined product. The mixture is pressed in the form of pellets which are sintered at 875°C for 16 h. The normalized resistance vs temperature plots are shown in figure 11. A representative XRD pattern is shown in figure 12.

2.5 *The $YBa_2Cu_3O_{7-\delta} + HgO + Ag$ system*

The implication of HgO as an internal source of oxygen to 123 systems is that this can be a successful technique for the preparation of Ag-clad tapes or wires through the usual powder-in-tube technique. This will do away with the problem of diffusion of oxygen into the core material through the silver barrier. However, there is possibility of a reaction of Hg with Ag during the sintering process. We, therefore, decided to do a preliminary experiment to add Ag together with HgO and see if the phase purity of the superconducting compound is maintained. To our great surprise we found that a very consistent value of $T_{c0} \sim 91$ K in all the specimens with 0·5, 1·0, 5·0, and 10·0 wt% Ag and HgO. For

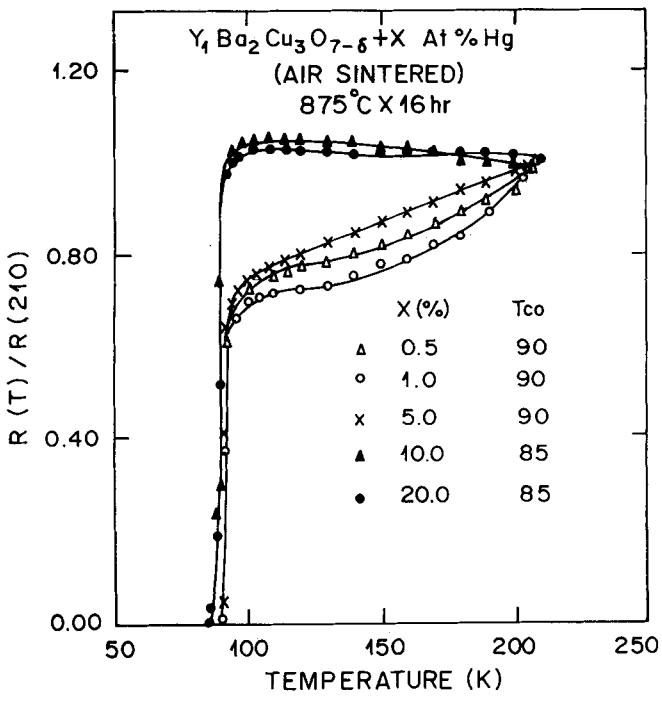

Figure 7. Resistive superconducting transition in $YBa_2Cu_3O_{7-\delta} + x$ at % Hg specimens for $x = 0·5$, 1·0, 5·0, 10·0, and 20·0. Very sharp and $T_{c0} \sim 90$ K is obtained for low x values (0·5, 1·0 and 5·0) (Pandey *et al* 1997).

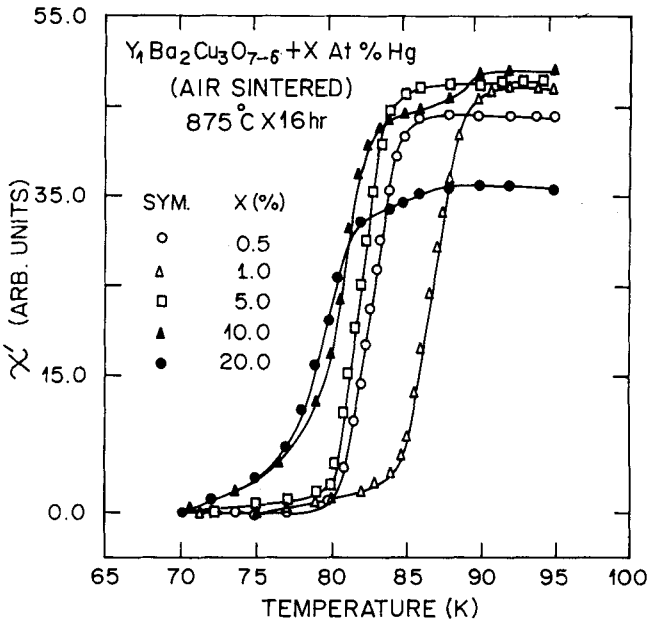

Figure 8. The real part (χ') of the ac susceptibility plotted against temperature for $YBa_2Cu_3O_{7-\delta} + x$ at% Hg specimens for the specimen $x = 20·0$ (Pandey *et al* 1997).

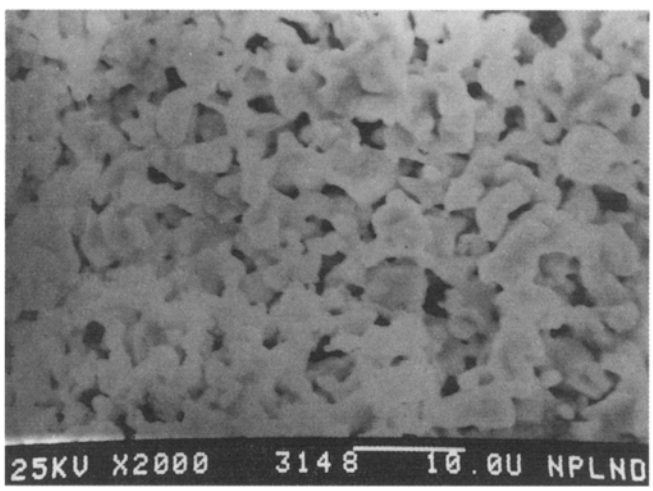

Figure 9. A typical SEM picture taken on the fractured surface for the specimen $x = 20·0$ (Pandey *et al* 1997).

20·0 wt% Ag and HgO, of course, T_{c0} dropped to ~ 84 K (figure 13). All the samples were sintered in air. This observation (Pandey *et al* 1998a) underscores the fact that HgO can be safely added to the powder even in the case of silver cladding which means that superconducting tapes can be prepared out of the powder prepared by HgO addition.

We have prepared superconducting tapes by powder-in-tube technique using the YBCO powder prepared by HgO addition. Standard steps of rolling with intermediate annealing at ~ 400–500°C have been followed for preparing the tapes. Finally, they were sintered at 850°C for ~ 16 h in air. From the resistivity vs temperature measurement the T_{c0} and the transition width were found to be ~ 90·5 K and ~ 4 K, respectively. It highlights that the processing can be greatly simplified as flowing oxygen is not required during sintering. It is also worthwhile to mention that the sintering temperature is reduced largely which again is quite advantageous. The oxygen contents estimated from the XRD data for the core material of tapes with 1·0 wt% HgO are found to be 6·99 and 7·00, respectively.

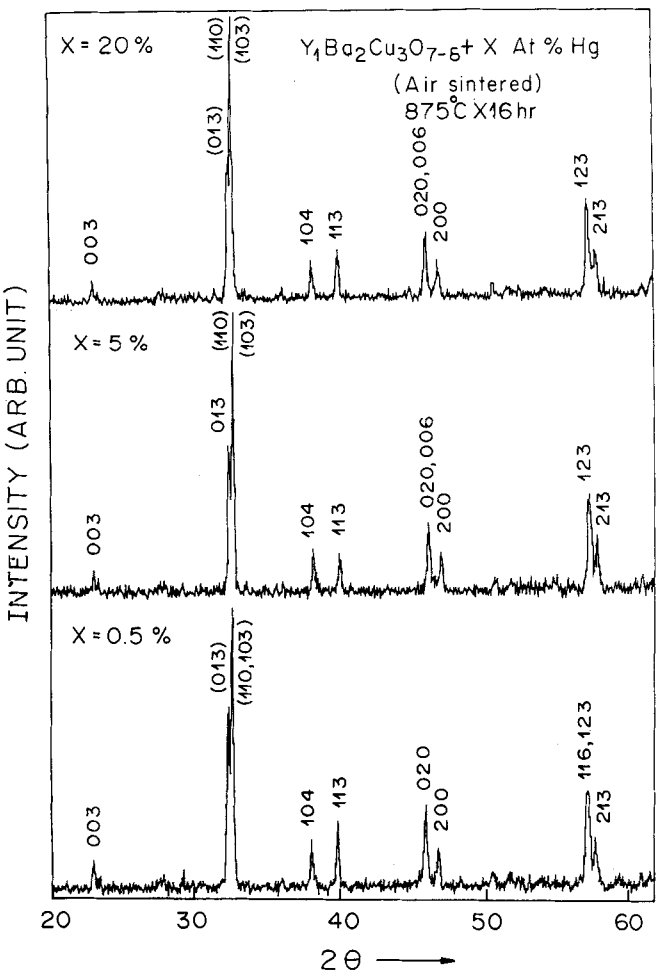

Figure 10. XRD spectra of $YBa_2Cu_3O_{7-\delta} + x$ at % Hg specimens with $x = 0·5$, 5·0 and 20·0 (Pandey *et al* 1997).

3. Intergranular flux creeping and magnetic relaxation

The problem of intergranular flux line dynamics within an array of disordered Josephson junctions has different ramifications. Apart from influencing the dissipation and behaviour of critical current in a granular medium, it can simulate the quantum particle transport scenario within a disordered medium (Oudenaarden *et al* 1996) which has been shown to be a generically different problem. The metal–insulator (or localization–delocalization) transition observed in the case of conduction in non-crystalline medium can be observed in the case of vortex transport in Josephson junction array as well. The naturally occurring array of grain boundaries within a ceramic superconductor bulk with large variation in the junction properties like junction resistance, critical current, coupling energy etc can be used for such studies.

We have studied the magnetic relaxation in these ceramic superconductors with and without silver within a low field regime (10–100 Oe) over a temperature range 20–77 K. A significant change in the pattern of magnetic relaxation rate is observed in the case of silver added samples. The relaxation appears to be much faster in the silver added samples. We have inverted the magnetic relaxation behaviour in order to calculate the distribution of the intergranular flux pinning energy U which, in fact, is a reflection of the distribution of the junction coupling energy as the flux pinning energy depends on the variation in junction coupling energy. The distribution is found to be narrower in the case of silver added samples. We have also derived semiquantitative relationships among the parameters like transport critical current density J_c, flux pinning energy U, and the transition width ΔT_c which are found to be followed by the experimental results.

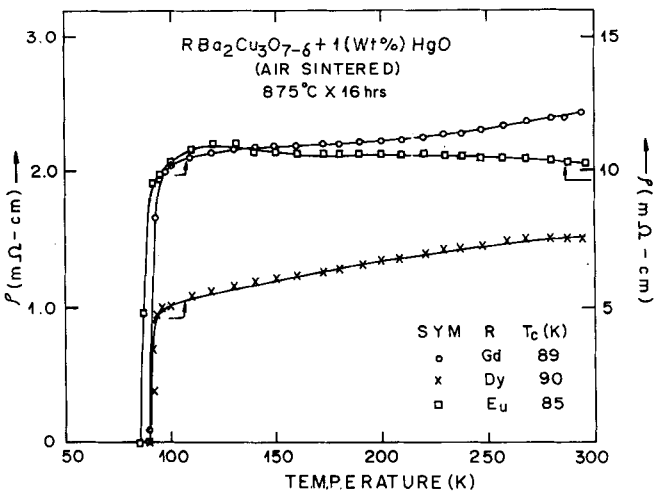

Figure 11. The resistivity vs temperature plots for $REBa_2Cu_3O_{7-\delta}$ + 1·0 wt% HgO air sintered (875°C, 16 h) where RE = Gd, Dy and Eu.

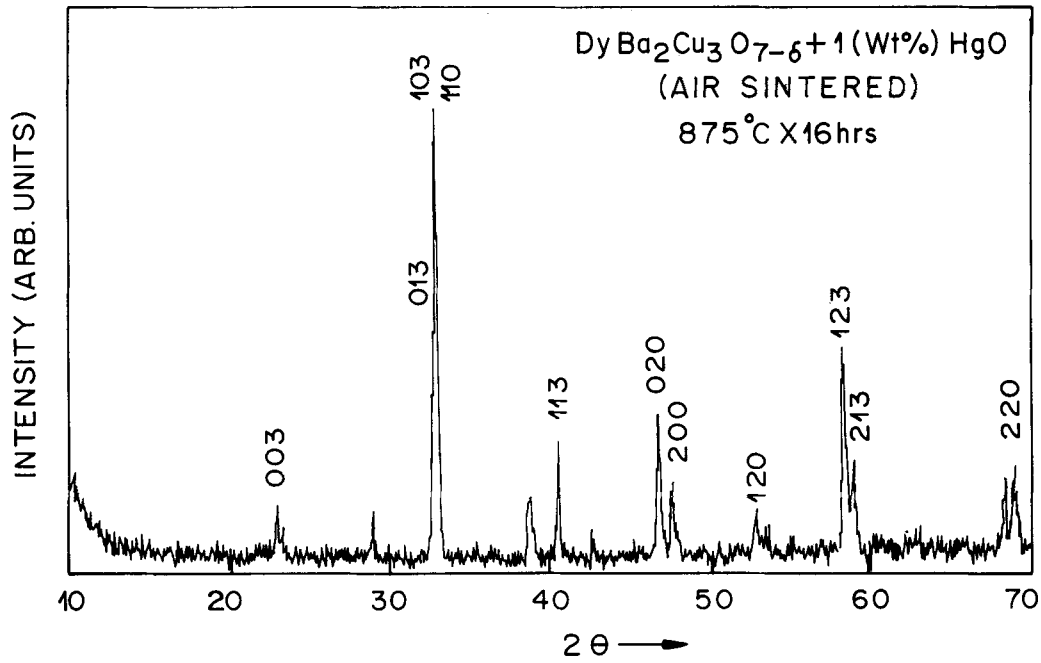

Figure 12. Representative XRD pattern for the $DyBa_2Cu_3O_{7-\delta}$ + 1·0 wt% HgO.

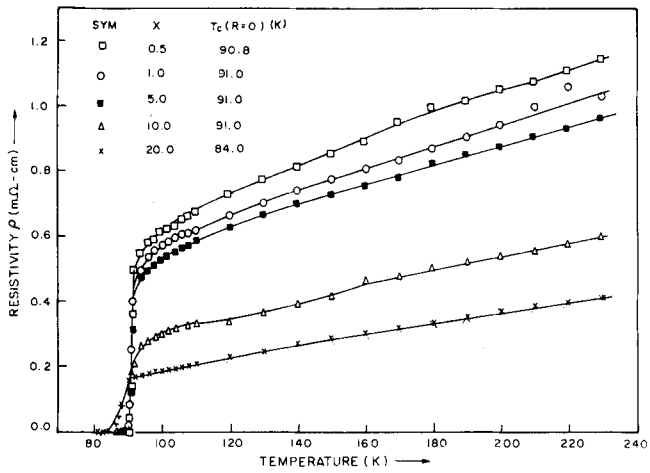

Figure 13. The resistive superconducting transition of $YBa_2Cu_3O_{7-\delta}$ + x wt% HgO + x wt% Ag for x = 0·5, 1·0, 5·0, 10·0 and 20·0.

3.1 *Magnetic relaxation studies*

Low field magnetic relaxation studies have been carried out in parent YBCO and BPSCCO superconductors as well as in 10–15 wt% silver added samples using a vibrating sample magnetometer (VSM; Model DMS 1660) coupled with a cryocooler of CTI, Cryogenics Inc. The steps followed for the relaxation studies are given below:

(i) The sample was cooled from room temperature to the desired temperature under zero field. Initial magnetization study was carried out on the virgin sample at that temperature over a field limit of 30–100 Oe. Such studies helped in identifying the intergranular critical fields: $H_{c1j}(T)$ and $H_{c2j}(T)$. In between these limits, the flux lines are present mostly at the grain boundaries while the grains remain shielded as diamagnetic inclusions.

(ii) Hysteresis loops were observed within the limit $H_{c1j}(T)$ and $H_{c2j}(T)$. The rate of field sweeping in both the initial magnetization and hysteresis loop studies were 0·15–0·2 Oe/s which, in turn, led to a magnetization variation rate ~ 7·0–10·0 × 10^{-4} emu/s. The corresponding electric field (E) was calculated (from London equation) to be ~ 10^{-8}–10^{-9} V/cm which was much smaller than the electric field criterion (~ 10^{-6} V/cm) used in the case of transport measurements. The impact of flux creeping, therefore, was severe on the magnetization which gave rise to sharp time decay in magnetization. A much faster field sweeping and emu variation, of course, can give rise to higher E but it will not allow a stable field profile within the sample.

(iii) The magnetic relaxation under a certain applied field which lies within $H_{c1j}(T)$ and $H_{c2j}(T)$ at a given temperature was studied over a time period of ~ 4000 s. Studies at different temperatures were carried out by recycling the sample through above T_c in order to drive out the remanent or trapped flux. In all these cases, the sample was brought back to the desired temperature under zero applied field.

The relaxation of the magnetization i.e. M vs t pattern was found to follow approximately logarithmic trend

over a time span of ~4000 s. The rate of magnetic relaxation $(1/M_0)\cdot(dM/d\ln t)$ (M_0 is the magnetization of the sample at the initial instant) vs temperature for all the samples are shown in figure 14. Clearly, the rate was faster in the case of silver added samples. By applying simple Anderson–Kim model

$$S = dM/d\ln t = -k_B T/U_0,$$

we calculated the flux pinning energy U_0. U_0 was found to be ~0·5 eV and 0·55 eV for the parent BPSCCO and YBCO sample, respectively while ~0·15 eV and 0·27 eV in the case of silver added samples.

We have also calculated the distribution of U from the experimentally observed relaxation behaviour following an inversion scheme (Hagen and Griessen 1989). Considering the distribution function $m(U)$ for the flux pinning energy and noting the basic Anderson-Kim magnetization equation, one can write

$$M(t,T) = M_0(T)\cdot[b(t)/a(t)]\cdot\int_0^\infty m(U)\times$$

$$[1-\{k_BT/U_0b(t)\}\ \ln\{1+(t/\tau)\}]\,dU, \qquad (1)$$

where the functions $a(t)$ and $b(t)$ ($t = T/T_c$) define the temperature dependence of M_0 and U_0 and τ is the characteristic relaxation time. By taking the derivative of this equation and evaluating $\ln(t/\tau)$ from the experimentally observed $M(t,T)$ and adjusting the functions $a(t)$ and $b(t)$ in order to arrive at temperature independent $\ln(t/\tau)$ we can suitably invert the expression (1) for evaluating the distribution function $m(U)$. Both the functions $a(t)$ and $b(t)$ are dependent on the coupling energy $E_J(T)$ and, therefore, follow $\sim(1-t)^n$ pattern.

The calculated patterns of $m(U)$ are shown in figure 15. Details of the calculations are available (Pandey *et al* 1998b). In the case of silver added samples, $m(U)$ becomes narrower with the shift in the U_m corresponding to the peak to the lower side. Therefore, it appears that the grain boundary characteristics become quite uniform in the case of silver added samples. Such uniformity leads to a higher current carrying cross-section within the sample and as a result of that the transport J_c improves. The relationship among the J_c, U and ΔT_c is discussed in the next subsection.

3.2 *Correlation among J_c, U and ΔT_c*

We have derived relationships among the transport J_c, flux pinning energy U, and the transition width ΔT_c by simple heuristic argument. The superconducting transition temperature ($T_c(R=0)$) for a two-dimensional ordered Josephson-junction array can be given by

$$k_BT_c(R=0) = \pi E_{J0}\ln(r_2/r_1), \qquad (2)$$

where the right hand side describes the total Josephson coupling energy for an ordered two-dimensional junction array (Lobb *et al* 1983). If we consider that corresponding to the junction coupling energy $E_{J0}+dE_J$, the transition temperature is $T_c(R=0)+dT_c$, we can write

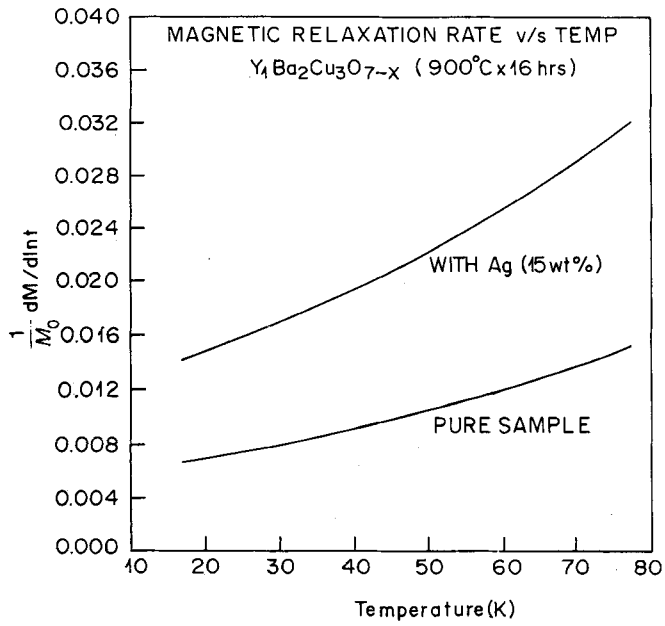

Figure 14. Representative normalized magnetic moment vs time plot for the parent as well as silver added sample.

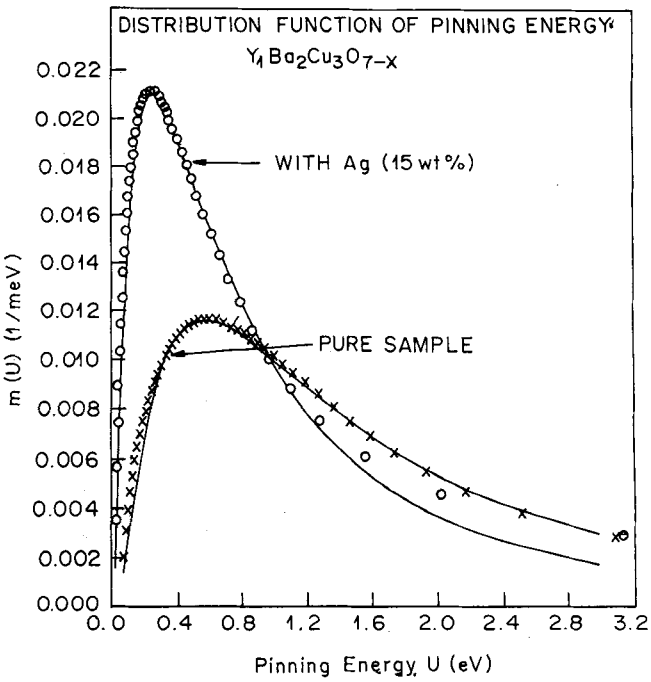

Figure 15. Representative plot of distribution function $m(U)$ of the flux pinning energy for the parent as well as silver added samples.

$$k_B [T_c(R=0) + dT_c] = \pi [E_{J0} + dE_J] \ln (r_2/r_1). \quad (3)$$

Dividing (3) by (2) and subtracting (1) from both the sides we obtain

$$\int_{T_{cmin}}^{T_{cmax}} dT_c/T_c(R=0) = \int_{E_{Jmin}}^{E_{Jmax}} dE_J/E_{J0},$$

which leads to

$$U = [E_{J0}/T_c(R=0)]\, \Delta T_c, \quad (4)$$

if we note that $U = (E_{Jmax} - E_{Jmin})$. Therefore, with the increase in the transition width, the flux pinning energy increases linearly. The transition width is determined by the variation in the junction coupling energy and can be taken as a measure of the degree of disorder. For a homogeneous junction network, the transition width is smaller. In order to derive a relationship between J_c and ΔT_c, we follow the calculations performed by Ambegaokar and Halperin (1969) regarding the vortex kinetics in a current-driven single overdamped Josephson junction. They have shown that the junction normal state resistance is given by

$$R/R_n = [I_0(U/k_BT)]^{-2},$$

where I_0 is modified Bessel function. Substituting U by (4) and noting the Ambegaokar and Baratoff (1963a,b) relationship between the critical current and junction resistance (which is found to be valid for all type of junctions—SIS, SNS, point contact etc (Prester 1998)), we can write

$$J_{c,min}/J_{c,max} = [I_0\{K \cdot \Delta T_c/T_c(R=0)\}]^{-2}, \quad (5)$$

where $K = E_{J0}/k_BT$, a dimensionless yet temperature dependent parameter. For large values of the argument,

$$J_{c,min} \approx J_{c,max} \exp[-K\Delta T_c/T_c(R=0)], \quad (6)$$

whereas the relationship turns quadratic if the argument is less than one. The experimentally observed pattern of J_c vs ΔT_c (where J_c is measured at 77 K) is plotted in figure 16 which can be fitted by (6) for the choice of the parameters $J_{c,max} \sim 200$ A/cm^2 and $K \sim 20$. The solid line in figure 16 represents the fit. It appears that for the same temperature one can expect to observe a cross-over from exponential decay of J_c to a quadratic decay for $\Delta T_c/T_c(R=0) \leq 0{\cdot}05$.

Silver addition leads to a higher degree of homogeneity which results in lower ΔT_c and hence higher J_c yet lower U. The reason behind apparent contradictory relation between J_c and U is the fact that the overall current carrying cross-section degrades with the increase in disorder and since the transport J_c under low-field depends more on the current carrying cross-section than on the flux creeping phenomenon, higher U appears to have given rise to lower J_c.

4. Conclusions

HgO addition/substitution turns out to be an extremely efficient technique to maintain proper oxygen stoichiometry within the entire bulk of the high-T_c superconductors even when the sample is treated in air. The substitution of Hg at Sr-site in the case of BPSCCO system and at Ba-site in the case of YBCO system reveals an improvement in T_c up to a substitution level $x = 0{\cdot}3$ and $0{\cdot}03$, respectively. Addition of HgO up to $1{\cdot}0$ wt % also leads to improvement in T_c. Higher level of addition gives rise to porous microstructure and hence broader transition width. HgO addition is found to be compatible with Ag as well since improvement in the superconducting properties is observed in Ag doped samples as well as in silver-sheathed superconducting tapes.

The low field (10–100 Oe) magnetic relaxation study reveals a faster intergranular flux creeping in the case of silver added samples. This is the result of much

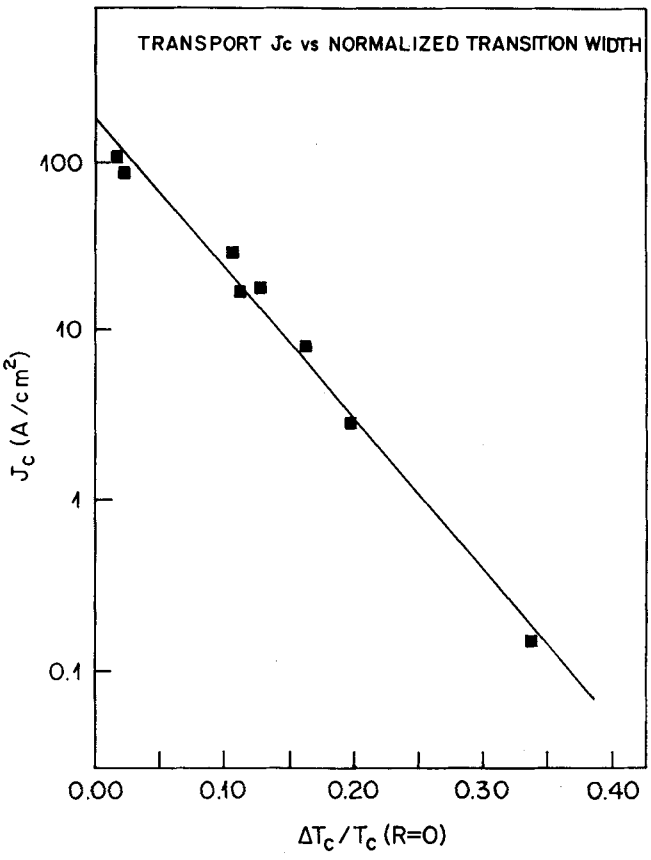

Figure 16. Variation of transport J_c with the normalized transition width. The solid line represents the fit.

uniformity in the grain boundary properties as a result of uniform distribution of silver along the grain boundaries all through the matrix. Such uniformity improves the current carrying cross-section. The transport J_c decays exponentially with the transition width ΔT_c which is a measure of the degree of disorder (inhomogeneity) within the matrix. The intergranular flux pinning energy U, of course, scales linearly with ΔT_c. Since by suitable silver addition one can control the degree of disorder within the sample, it turns out that it is possible to reach an optimum combination of the parameters J_c, U and ΔT_c: high J_c, high U and low ΔT_c.

References

Ambegaokar V and Baratoff A 1963a *Phys. Rev. Lett.* **10** 486

Ambegaokar V and Baratoff A 1963b *Phys. Rev. Lett.* **11** 104

Ambegaokar V and Halperin B I 1969 *Phys. Rev. Lett.* **22** 1364

Conder K, Rusiecki S and Kaldis E 1989 *Mat. Res. Bull.* **24** 581

Hagen C W and Griessen R 1989 *Phys. Rev. Lett.* **62** 2857

Kao Y H, Yao Y D, Jang L Y, Xu F, Krol A, Song L W and Sher C J 1990 *J. Appl. Phys.* **67** 353

Lahiry S, Reddy Y S, Sarkar B, Rajput R, Suri D K, Sharma R G and Sharma B B 1994 *Physica* **C225** 207

Lobb C J, Abraham D W and Tinkham M 1983 *Phys. Rev.* **B27** 150

van Oudenaarden A, Vardy S J K and Mooij J E 1996 *Phys. Rev. Lett.* **77** 4257 and all the relevant references therein.

Pandey A, Rajput R, Sarkar B, Reddy Y S and Sharma R G 1996 *Physica* **C256** 335

Pandey A, Reddy Y S and Sharma R G 1997 *J. Mater. Sc.* **32** 3701

Pandey A, Rekhi S and Sharma R G 1998a *J. Mater. Sc. Lett.* (in press)

Pandey A, Bhattacharya D and Sharma R G 1998b *Phys. Rev.* **B** (submitted)

Prester M 1998 *Supercond. Sci. Tech.* **11** 333 and all the relevant references therein.

Putilin S N, Antipov E V, Chmaissem O and Marezio M 1993 *Nature (London)* **362** 226

Samel P K *et al* 1995 *Indian J. Phys.* **A69** 45

Schilling A, Cantoni M, Guo J D and Ott H R 1993 *Nature (London)* **363** 56

Singh J P, Leu H J, Poeppel R B, van Voorhees E, Goudey G T, Winsley K and Shi Donglu 1989 *J. Appl. Phys.* **66** 3154